CCD photometry tests for a mission to detect Earth-size planets in the extended solar neighborhood

D. G. Koch[a], W. Borucki[a], E. Dunham[b], J. Jenkins[c], L. Webster[d], F. Witteborn[e]

[a]NASA Ames Research Center, MS 245-6, Moffett Field, CA 94035
[b]Lowell Observatory, 1400 W. Mars Hill Rd, Flagstaff, AZ 86001
[c]SETI Institute, 2035 Landings Dr., Mountain View, CA 94943
[d]NASA Ames Research Center, MS 244-14, Moffett Field, CA 94035
[e]Orbital Sciences Corp, MS 245-6, Moffett Field, CA 94035

ABSTRACT

The thirty or so extrasolar planets that have been discovered to date are all about as large as Jupiter or larger. Finding Earth-size planets is a substantially more difficult task. We propose the use of spacebased differential photometry to detect the periodic changes in brightness of several hours duration caused by planets transiting their parent stars. The change in brightness for a Sun-Earth analog transit is $8x10^{-5}$. We describe the instrument and mission concepts that will monitor 100,000 main-sequence stars and detect on the order of 500 Earth-size planets, if terrestrial planets are common in the extended solar neighborhood.

We have performed and will discuss end-to-end laboratory measurements that demonstrate the feasibility of differential photometry under realistic operating conditions. The tests included a realistic star field in which individual transits can be generated, fast optics with a realistic point spread function, and a flight-type back-illuminated CCD. Spacecraft motion was simulated using piezoelectric transducers. Data acquisition and processing used the same methods as planned for the space mission. A system-level differential-photometric precision of 10^{-5} has been demonstrated under realistic conditions.

Keywords: extrasolar planets, Earth-size planets, photometry, CCDs, planetary transits

1. INTRODUCTION

Both NASA and ESA are considering major investments to obtain the spectra of extrasolar planetary atmospheres in order to search for evidence of life. The eventual success of that enterprise depends to a great extent on the frequency of Earth-size planets, i. e., the number of planets per star. Knowledge of this will assist in scoping the enterprise for detection and characterization of nearby planetary systems.

Transit photometry has already contributed to the characterization of giant extrasolar planetary atmospheres[1] and provided an independent means of detection. Based on the transit method, we have developed, refined and proposed a space mission with the sensitivity and precision needed to determine the frequency of Earth-size planets in the extended solar neighborhood[2, 3]. At the heart of the mission is an array of CCDs used to continuously measure the relative brightness variations of 100,000 main-sequence stars for transits.

A Testbed Facility has been constructed to demonstrate that under realistic operating conditions with all known confounding factors that could introduce noise, differential ensemble photometry using CCDs can repeatedly and reliably measure transit signals due to Earth-size planets. The Testbed Facility includes: a simulated star field with an approximately solar spectrum, fast optics to simulate the spaceborne telescope, a thinned back-illuminated CCD similar to those to be used on the spacecraft operating at 1 megapixel per second read rate, and shutterless operation. The Testbed Facility is thermally and mechanically isolated. Each source of noise is introduced in a controlled fashion and evaluated. Pointing noise or changing thermal conditions in the spacecraft can cause star-image motion at the millipixel level. These motions are imposed by piezoelectric devices, that move the CCD photometer relative to the star field. Transit signals as small as Earth-size transits of solar-like stars are generated and measured. This is accomplished by electrical self-heating and expansion of fine wires placed across many of the star apertures. The small decrease in stellar brightness is used to demonstrate that Earth-size planets can readily be detected under realistic noise conditions and at the shot-noise-limited level. The effects of imposing multiple noise sources are shown and the resulting detectability of planets is presented.

Part of the SPIE Conference on UV, Optical and IR Space Telescopes and Instruments • Munich, Germany • March 2000
SPIE Vol. 4013

2. SCIENTIFIC GOALS AND OBJECTIVES OF THE *KEPLER MISSION*

The centuries-old quest for other worlds like our Earth has been rejuvenated by the intense excitement and popular interest surrounding the discovery of giant planets like Jupiter orbiting stars beyond our Solar System. Other than the pulsar planets, all of the extrasolar planets detected to date are roughly as massive or more so than Jupiter. The challenge now is to find planets which are 30-600 times less massive than Jupiter. **The *Kepler Mission* is specifically designed to survey the extended solar neighborhood to detect and characterize hundreds of Earth-size and larger planets in or near the habitable zone.** The scientific goal of the *Kepler Mission* is to explore the structure and diversity of planetary systems. This is achieved by an unbiased survey of a large sample of stars to:

- Determine the frequency of 0.8 $R_\oplus$ and larger planets in or near the habitable zone of a wide variety of spectral types of main-sequence stars;
- Determine the distribution of sizes and orbital semi-major axes of these planets;
- Estimate the frequency of planets orbiting multiple-stellar systems;
- Determine the distributions of orbits, albedo, size, mass, and density of short-period giant planets;
- Identify additional members of each photometrically-discovered planetary system using complementary techniques;
- Determine the properties of those stars that harbor planetary systems.

2.1. Photometric detection of extrasolar planets

Transit signals by Earth-size planets in orbit around solar-like stars produce a relative brightness change of 8×10^{-5} and have durations from 4 to 16 hours for planets in or near the habitable zone. The brightness change is simply the ratio of the area of the planet to the area of the star. From orbital mechanics and a knowledge of the mass-radius relationship of main-sequence stars, the central-transit time is given by:

$$t_c = 13.1 d^* \sqrt{R / M^*} \cong 13.1 \sqrt{R} \text{ hours}, \quad (1)$$

where t_c is the central-transit time in hours, d^* is the stellar diameter in solar units, R is the semi-major axis in AU and M^* is the stellar mass in solar masses. For a transit to be visible, the orbital plane must be nearly aligned along the line-of-sight to the star. The probability for this to occur is d*/2R, the diameter of the star over the twice the semi-major axis of the orbit. For the Sun-Earth analog this is 0.5%, since d^* is about 0.01 AU and R is 1 AU.

Three or more transits, all with a consistent depth, duration and temporal spacing are necessary to definitely detect a planet using the transit method. Each transit requires sufficient statistical significance, so that the depth, the duration and the temporal spacing can be used to discriminate between random events and real transits. For transits with greater than minimum signal to noise the shape of the transit can be used as a further distinguishing signature of a transit. The photometer must be spaceborne to obtain the necessary precision and to avoid interruptions caused by diurnal and seasonal cycles.

The size of the planet is determined from the apparent change in brightness and a knowledge of the stellar diameter. The orbital semi-major axis can be derived from the orbital period, a knowledge of the stellar mass and the application of Kepler's third law. The planet's characteristic temperature can then be calculated given the orbit, the stellar temperature and assuming the planet to be a black body.

2.2. Observing plan and expected results

Assuming all main-sequence stars have planets and excluding binary star systems with orbits similar to habitable planets, one must continuously and simultaneously observe of order 100,000 main-sequence stars to detect several hundred planets, since the probability for detection of any single system is on the order of 0.5%. To do this, a single rich field of 84 deg^2 of the Milky Way in the Cygnus region will be observed for four years. In total we expect to detect on the order of 2300 planets with the *Kepler Mission.* A detailed description of the mission has been given elsewhere[2, 3].

3. TECHNOLOGY DEMONSTRATION TESTBED

The *Kepler Mission* depends on the ability to reliably measure the very small relative change in brightness of a star caused by the transit of an Earth-size planet. We have constructed a high-fidelity Testbed Facility of the end-to-end photometry system. This has been used to show that under all of the expected operating conditions, which can add noise to the measurement, the signature of an Earth-size transit is readily detectable.

The Testbed Facility (Figure 1) has been built to simulate the elements that will compose the flight system:

- A simulated star field that represents all of the features of the real sky that are important for ensemble photometry;
- A photometer that has the same characteristics as the flight photometer, including:

- Fast optics to focus the star field onto the CCD detector,
- A commercially available CCD that could be used in the flight system,
- High speed readout electronics (operating at 1 megapixel/sec) to process the data as if onboard the spacecraft, and
- Ground software used to produce the light curves, detect transits and evaluate the precision of the data;

• A structure that provides thermal, mechanical and RF isolation from the laboratory environment.

The objective of the technical demonstration was to show that this end-to-end system can maintain the required relative precision over a period of time necessary to detect transits when all of the confounding noise factors are included. Note that the critical parameter is only relative precision, that is, the variation in the ratio of the flux of one star to the fluxes of many nearby stars read at the same time on the same CCD.

The major subsystems that comprise the Testbed Facility are shown in Figure 1. The Source simulates the sky and:

• Produces the same flux as the stars in the 9th to 14th magnitude range as will be measured with the Kepler photometer,
• Has a similar spectral color to the Sun,
• Has the same star density as the Cygnus region to be observed in the mission down to 19th magnitude stars,
• Has several 4th magnitude stars, and
• Has the ability to generate Earth-size transits for selected stars.

The Camera simulates all of the functions to be performed by the Kepler photometer. It consists of:

• Fast optics with a central obscuration,
• A flight-type CCD without a shutter,
• CCD controller electronics,
• Control and data acquisition computer and software, and
• A CCD cooling system.

The data are read out every 3 seconds and co-added to form either 3-minute or 15-minute integrations. The Testbed Facility also incorporates: piezoelectric transducers (PZT) to provide motion similar to that modeled for the spacecraft jitter and a super-invar metering truss to maintain pointing stability between the camera/PZTs and the star plate. There is a thermal enclosure made of 6-mm thick aluminum with 5-cm thick insulating foam. The enclosure is actively controlled using thermal electric coolers/heaters (TEU). The aluminum plates also serve as an RF shield. Baffling between the star plate and the Camera excludes stray light and maintains cleanliness.

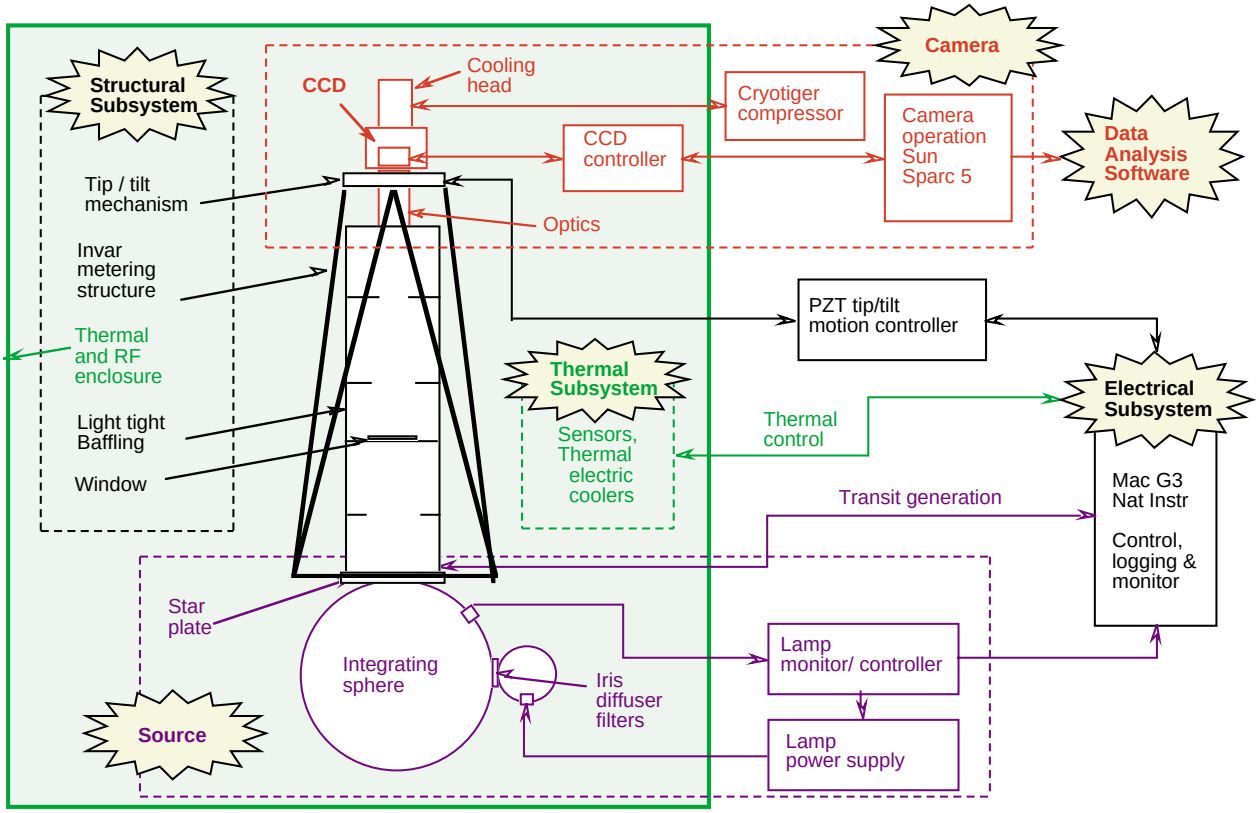

Figure 1. Kepler Testbed system architecture

For these tests a Marconi 42-80 (formerly EEV) back-illuminated CCD was selected. This device is an excellent candidate for the *Kepler Mission.* The CCD has 2048x4096 pixels of 13.5 µm. The overall size is 27x54mm. The pixels are binned 2x2 on the CCD to 27µm. In effect it is being used as a 1024x2048 device. Throughout the rest of the paper when reference is made to pixels, it is to binned pixels. The binning improves both the readout speed and the photometric precision by providing a well-depth of about 600,000 electrons. A binned pixel is 3.6 arcsec both in the lab and for the mission. The device is read out at 1 megapixel/sec through two separate amplifiers. About half of the CCD is illuminated by the star plate.

3.1. Test capabilities

An earlier set of laboratory tests has shown that under nominal operating conditions without inclusion of confounding effects the desired precision was achievable[4,5]. There are many confounding factors that influence the end-to-end system noise and hence the detectability of transits. The purpose of this Testbed was to: 1) include the effects of all realistic noise sources, 2) identify the optimal operating conditions under the influence of each confounding factor and 3) show that when all of the effects are taken together, Earth-size transits can be reliably observed. The Testbed Facility incorporates the ability to control and measure the following effects on the noise performance of the system:

1. Temperature — Operate the CCD between -60°C to –40°C;
2. Focus change: — Vary the focus (point spread function size);
3. Thermal effects — Provide active thermal control of all elements to permit isolation of thermal effects;
4. Photometric aperture — Investigate the use of various photometric apertures;
5. Dynamic range — Simultaneously provide target stars with m_V=9 to 14;
6. Crowded field — Operate with a background star density similar to the real sky with stars as faint as m_V=19;
7. Smearing — Operate without a shutter during readout with other stars in the same CCD column;
8. Field rotation — Shift the star field to different parts of the CCD to simulate spacecraft rotation every 3 months;
9. Bright stars — Provide bright stars with m_V=4 in the field-of-view;
10. Spacecraft jitter — Provide motion up to 500 millipixels (expect ±3 millipixels) at various frequencies and amplitudes;
11. Cosmic rays — Simulate with software the effects of cosmic-ray hits on the CCD;
12. Stellar variability — Simulate with software the effects of stellar variability at the relevant frequencies; and
13. Transits — Create transits for selected stars in the range m_V=9 to 14.

3.2. Performance criteria

To meet the goals and objectives of the *Kepler Mission* as described above the spacecraft/photometer design criteria for an acceptable one-sigma total noise level has been established as $2x10^{-5}$ or 0.25 Earth-area for an m_V=12 star in five hours of observing. These parameters are listed in the bottom of Table 1. The total noise includes: photon-shot noise ($1.4x10^{-5}$), instrument noise ($1x10^{-5}$) and stellar variability ($1x10^{-5}$). The signal is determined by the photometer collecting area and system efficiency. In line 1 of Table 1 the signal for various stellar magnitudes is scaled from a 12th magnitude star. The shot noise (Table 1, line 2) is the square root of the measured signal (line 1). The fractional instrument noise (all noise sources except photon-shot noise and stellar variability) is converted to an absolute noise and given in line 3. The shot and instrument noise are combined as a root-sum-square (RSS) and given in line 4. The fractional noise in line 5 is the ratio of line 4 to line 1. Stellar variability (line 8) is a given for any particular star. For the Sun and presumably other solar-like stars it is less than $1x10^{-5}$ at the relevant temporal frequencies and spectral bandpass. The total fractional noise (line 10) is obtained by an RSS combination of lines 5 and 8. The total noise relative to an Earth-size transit is line 9 divided by $8x10^{-5}$. For a 12th magnitude star this is 0.25. The reciprocal of the total noise gives the number of sigma for a one-Earth transit (line 11).

The performance reported in §4 for the Testbed is to be compared to the values given in bold in line 5. The better performance shown for 9th, 10th, and 11th magnitude stars is not required, since the objective of the *Kepler Mission* is to detect Earth-size planets. The required performance at these brightnesses is taken to be the same as for 12th magnitude stars.

3.3. System characterization

Prior to establishing a baseline performance without inclusion of all the confounding factors, a number of tests were performed to characterize the system. These included testing the effects of items 1 through 4 in the capabilities list (§3.1).

3.3.1. Operating temperature

The CCD was operated at temperatures of –40°, -50° and –60°C and the dark current and its effects on the noise measured. Going from –40°C to –50°C reduced both the dark current and the system noise. Below –50°C there was no improvement in the system noise. At –50°C the dark current no longer dominated other noise sources. A temperature of –50°C was used for all of the test results reported here.

Table 1 Performance Criteria Based on the Design Parameters

Stellar magnitude	9	10	11	12	13	14	units	line
Shot and instrument noises								
Signal (e^- in X hrs) (1) and (2)	8.00E+10	3.00E+10	1.25E+10	5.00E+09	2.00E+09	8.33E+08	abs	1
Shot noise (e^- in X hrs)	2.83E+05	1.73E+05	1.12E+05	7.07E+04	4.47E+04	2.89E+04	abs	2
Instrument absolute noise (e^- in X hrs) (3)	5.00E+04	5.00E+04	5.00E+04	5.00E+04	5.00E+04	5.00E+04	abs	3
RSS shot and instrument (e^- in X hrs)	2.87E+05	1.80E+05	1.22E+05	8.66E+04	6.71E+04	5.77E+04	abs	4
Fractional noise (RSS noise/signal)	3.59E-06	6.01E-06	9.80E-06	**1.73E-05**	**3.35E-05**	**6.93E-05**	frac	5
Relative noise (Earth area transit) (4)	0.04	0.08	0.12	0.22	0.42	0.87	rel	6
SNR for one-Earth (1/previous line)	22.28	13.31	8.16	4.62	2.39	1.15	σ	7
Shot, instrument noises and stellar variability:								
Stellar variability (fractional) (5)	1.00E-05	1.00E-05	1.00E-05	1.00E-05	1.00E-05	1.00E-05	frac	8
RSS stellar and fractional noise	1.06E-05	1.17E-05	1.40E-05	2.00E-05	3.50E-05	7.00E-05	frac	9
Total rel noise (Earth area transit) (4)	0.13	0.15	0.18	0.25	0.44	0.88	rel	10
SNR for one Earth (1/previous line)	7.53	6.86	5.71	4.00	2.29	1.14	σ	11
Parameters used to define the design criteria:								
(1) Signal for m_V=12 star		1.00E+09					e/hr	
(2) Integration time = X		5					hrs	
(3) Instrument noise limit (for m_V=12 in 5 hrs)		1.00E-05					frac	
(4) One-Earth area transit		8.00E-05					frac	
(5) Stellar variability		1.00E-05					frac	

3.3.2. Focus and point spread function

The star images have intentionally not been made into sharp unresolved points of light on the CCD. The point spread function is intentionally extended over many pixels for two reasons: 1) to reduce the sensitivity of the photometric precision to subpixel variations in quantum efficiency when there is motion and 2) to provide an adequately large integrated well depth to prevent saturation. An optimum focus was found wherein a 5x5 pixel aperture contained 80% of the energy and about a 3-pixel diameter contained 40% of the energy. This focus was used throughout the remainder of the tests reported here.

3.3.3. Thermal effects and uncorrected signal variation with motion

A limitation to the photometric precision of aperture photometry comes from the spatial stability of the Point Spread Function (PSF) relative to the aperture. Two effects take place as the PSF moves within the aperture: 1) the gains and losses of the PSF at the edges of the aperture are never equal at some level of precision and 2) the detector may also have significant spatial variations at the pixel or subpixel scale in quantum efficiency. There are two types of motion to consider: random motions that have a mean of zero over the long term and drifts that cause a change in the mean position over the long term. Long term is meant to refer to time scales on the order of expected transits. For transit times of two hours to 16 hours, this implies the mean motion needs to be stable on time scales of 40 minutes to two days. What is stable? If the total for instrument noise is to be less than 10^{-5}, then changes caused by either variations in the mean position due to random motion not averaging out or a drift of the mean position after any corrections need to be less than or on the order of $0.5x10^{-5}$.

Small long-term changes in the temperatures of the CCD and its internal mount, and the wall and base of the CCD dewar, were found to significantly affect the spatial stability of the images. In addition to an actively controlled thermal enclosure for the entire Testbed (Figure 1), proportional temperature control was instituted for these components and for the CCD electronics box. This permitted identification and mitigation of thermal effects of these components.

Tests were conducted to measure the effect of motion at the millipixel level on the amplitude of the signal. The results are presented in Figure 2. An initial test was performed using a polycarbonate holographic diffuser, which produced a smooth beam that had a full-width of 7.4 pixels at the 20% intensity point. (The diffuser was not used in any other tests.) The motion in x and y of the camera is shown in panel a as a function of time. The total motion is 500 millipixels. Panel b shows the change in amplitude with time for eight different stars scattered over the CCD for the motion in panel a. The relative amplitudes are highly correlated with an amplitude variation of up to 10^{-4} per one millipixel of motion similar to what has been reported previously[4, 5]. Panel c shows the superposition of motion of each star relative to each star's central pixel. For motion near the center (star 5) or tangent to the center (stars 6 and 13) there is very little variation. For motion radially from the center the amplitude increases while moving towards the center and decreases for motion away from the center. The gradient increases with increasing distance from the center (compare stars 5 and 11). A second test was performed using the optimum PSF (§3.3.2) without the diffuser. Figure 2d shows the x and y motion versus time, panel e shows the amplitude variation and panel f shows the superimposed positions of the PSF relative to the centers of each stars aperture. For this case

a 5x5 aperture was used which is close to optimum for the fainter stars (see the next section). Panels g, h, and i are from the same test but for 9th magnitude stars using 11x11 apertures. The response in all cases can be explained as a result of the wings of the PSF moving in and out of the aperture.

Calculations were performed to quantify the signal amplitude changes for motions at the one-millipixel level. For these calculations we assumed the quantum efficiency is uniform throughout the entire photometric aperture and effects of shot noise were not included. Hence, an analytic form using a Gaussian, could be used for the integrations. The distribution of energy near the peak of the PSF (uniform, spiky, etc.) contributes a constant amount and therefore is not relevant. The only variance will be due to the wings of the PSF moving relative to the edges of the aperture. The integrations were performed numerically. The results reproduce the behavior shown in Figure 2 and give comparable amplitude variations with motion, thereby confirming the interpretation of the effects.

Thus long-term drifts in the mean stellar positions at the millipixel level are significant and undesirable. However, these variations being highly correlated, as shown in Figure 2, are correctable and the corrections have been incorporated in the data analysis program *decorr*[6] used for decorrelating normalized fluxes

3.3.4. Aperture photometry

Aperture photometry is one choice for measuring the amplitude of the flux versus time. Point Spread Function (PSF) fitting would be another method, but is much more computationally intensive and requires a good knowledge of the PSF. The size of the aperture chosen relative to the PSF along with the amplitude of the shot-noise relative to other noise sources affects the measured noise. Using the optimum PSF (§3.3.2), the noise was measured as a function of the aperture size in pixels for each

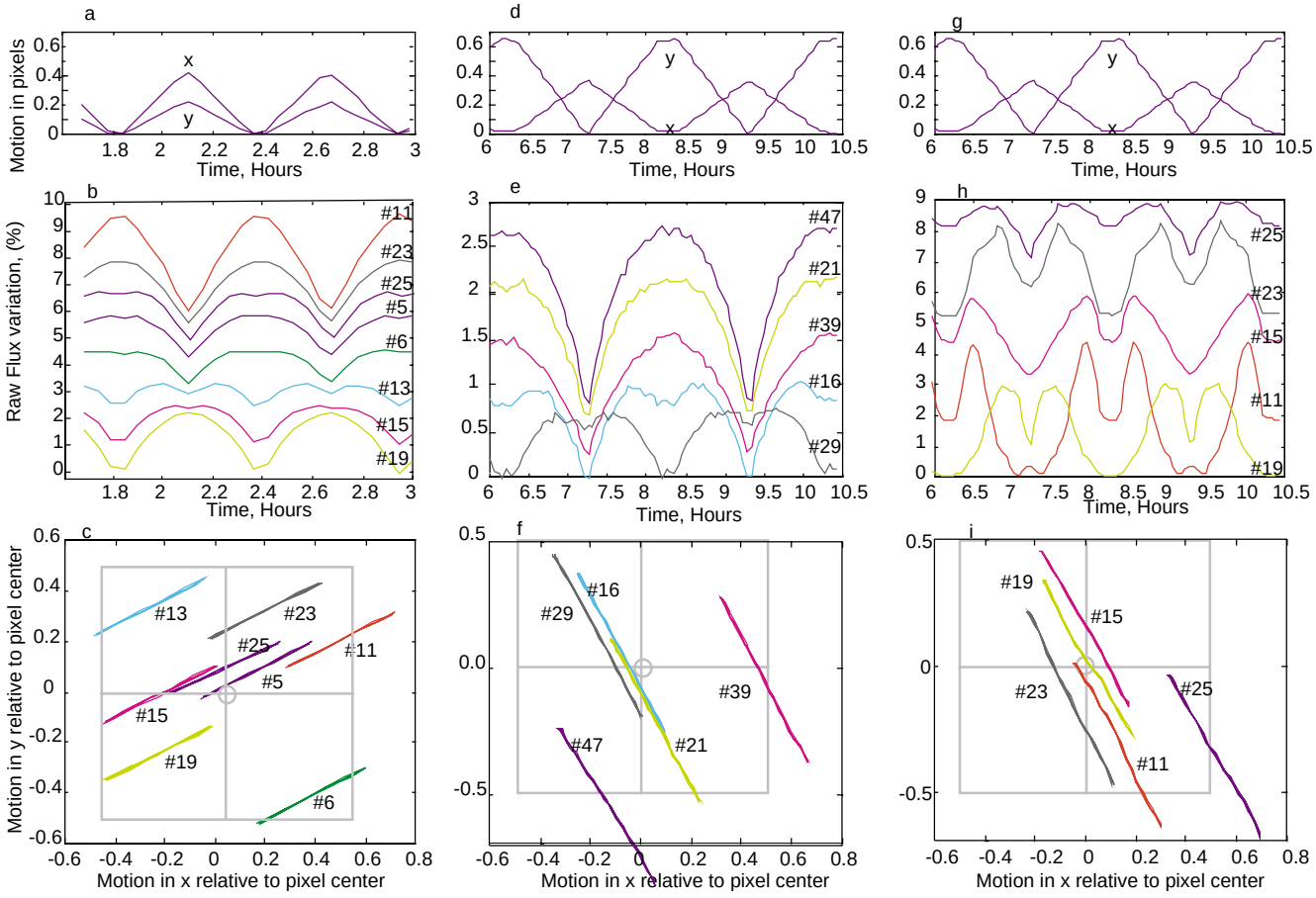

Figure 2. Uncorrected Signal Variation with Motion. Motion in x and y of the CCD is shown in panels a, d and g as a function of time. Panels a, b and c are from a test with a diffuser in the beam producing a broad smooth PSF. Panels d, e and f are for 12th and 13th magnitude stars and a 5x5 pixel aperture without the diffuser. Panels g, h and i are for 9th magnitude stars and a 11x11 pixel aperture without the diffuser. Panels b, e and h show the change in amplitude with time. Panels c, f and i show the superposition of motion of each star relative to each star's central pixel.

stellar magnitude and is given in Table 2. The one-sigma noise is given in units of an Earth-area transit. The maximum allowable noise is from Table 1 line 6. It is evident that for brighter stars (m_V=9) the noise is minimized with the use of a larger aperture where the instrument noise is small relative to the shot-noise (compare lines 2 and 3 in Table 1). For the fainter stars, the outer pixels of a large aperture become dominated by instrument noise and contribute insignificantly to the measured value. The optimum aperture for each magnitude is shaded in Table 2. These results are, to first order, an effect achieved in optimum pixel weighting, which is part of the analysis software[6] that reduces the photometric errors produced by short-term motions.

Table 2 Measured Noise (Earth-area)

m_V	Pix=5	=7	=9	=11	Max allow
9	0.19	0.11	0.09	0.08	0.22
11	0.15	0.11	0.10	0.11	0.22
12	0.22	0.16	0.18	0.18	0.22
13	0.36	0.33	0.33	0.34	0.42
14	0.57	0.52	0.66	0.78	0.87

3.4. Data processing and analysis

The flow of the data processing and analysis is illustrated in Figure 3. The test conditions (one or several listed in §3.1) are defined external to the data system. The operation of the CCD and acquisition of the data are performed with Lowell Observatory Instrument System[7] (LOIS). LOIS is an interface to the CCD controller[8]. To prevent saturation the CCD is readout every three seconds at one megapixel per second using two amplifiers. During readout the pixels are binned 2x2 on the chip to simulate use of a CCD with larger pixels. There is no shutter in the system. Each image is co-added for either 3 or 15 minutes and then written to disk as a FITS file. The effect of cosmic rays can be simulated by using software to inject them into the individual three-second readouts. They can then either be left in the data or removed by a separate software module. At the end of the run the data are archived onto DLT tape.

During the *Kepler Mission* the full images are not telemetered to the ground. Rather the pixel data for each star being monitored are extracted on-board after each 15-min co-add to produce one sample in time of each star's light curve. The software module *Space3* performs this function. It produces several files in the Testbed allowing for a choice of further processing to be performed. Simulated stellar variability can be added to any of these files as desired. Raw pixel data are used by the program *optflux*, which uses optimal pixel weighting, rather than equal weights to reduce the sensitivity to motion. The best results are obtained by pre-screening the pixels and including only those pixels that contribute significant statistical information to the flux calculation. This is a way to choose the appropriate photometric aperture based on the stellar

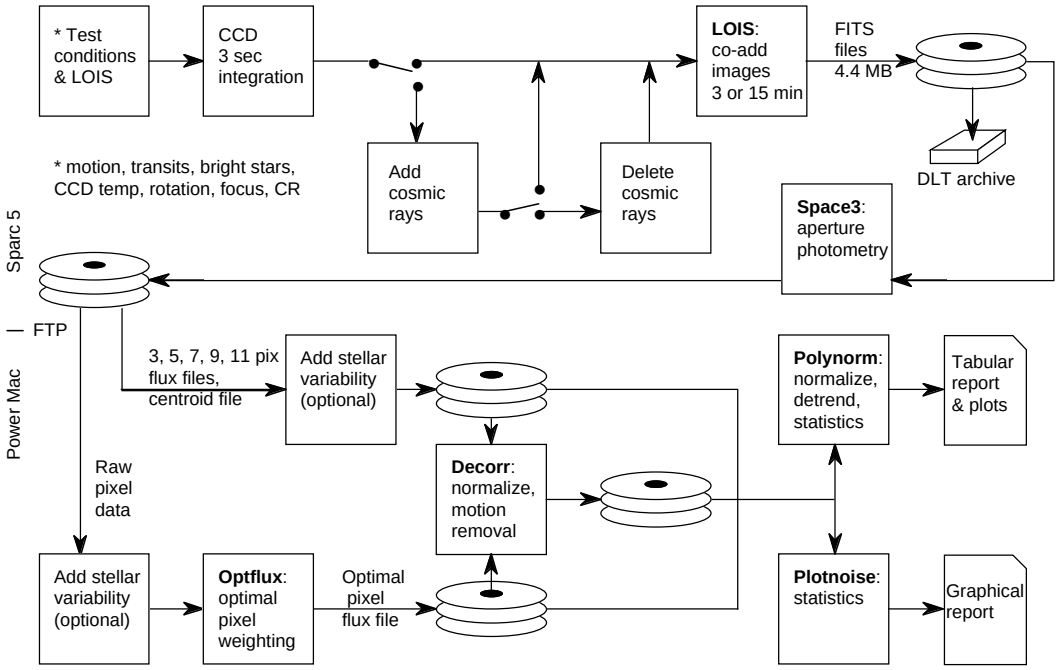

Figure 3. Data Flow and Processing Steps

brightness (see §3.3.2), the location of the PSF relative to the fixed pixel grid and account for noise and structure in the background[6]. The program *optflux* produces a flux file identical in format to the other flux files produced by *Space3*. A single flux file constitutes what is telemetered to the ground during the mission.

The program *decorr* removes any time-varying component in the relative fluxes that is highly correlated, thereby mitigating the effects of long-term drifts in the centroids. During the mission this process will be performed on the ground. The result is light curves for each star for each point in time. The results of the analysis are summarized by either the program *polynorm*, which provides a tabular summary of the test (see Table 3) that can be compared to the values in Table 1 or *plotnoise,* which provides a graphical summary (Figure 4).

4. TEST RESULTS

4.1. Baseline test and generalities in the data interpretation

Prior to introducing external confounding factors, the effects of several common factors were measured in a Baseline test, since these are incorporated in the star plate. These included: dynamic range (§3.1, item 5), crowded field (§3.1, item 6) and smearing (§3.1, item 7). The typical test duration was about 48-60 hours, except for the long duration test, which ran for more than ten days. The results of the Baseline test are presented in Figure 4a.

Each panel in Figure 4 contains the information for the 138 stars that are measured in each test. The noise is presented in terms of the one-sigma precision over a five-hour integration. The solid line is the maximum allowed instrument plus shot noise and is based on line 5 of Table 1. The circles present the measured noise for each individual star that does not have a wire. The Ws are the measured noises for those stars that have transit wires (see §4.5). The x is the shot noise calculated for each star. The + is an estimate of the background for each star, based on the background measured in a blank area of the CCD. A common feature seen in all of the tests is that almost all of the stars that are above the max-allowed line (the Ws) are 9^{th}, 12^{th}, and 14^{th} magnitude stars with transit wires. Whereas those without wires (the Os), which includes all of the 11^{th} and 13^{th} magnitude stars almost always remain below the max-allowed line. It is apparent that the wires add extra noise and can therefore be justifiably ignored when evaluating the system noise.

4.2. Rotation-translation

The spacecraft will be rotated 90° about the photometer axis every three months to maintain the side of the spacecraft with the solar panels pointed towards the Sun and the opposite side with radiator panels pointed to deep space. In between these rotations the spacecraft attitude remains fixed with the solar-vector slowly rotating through only a single quadrant of the spacecraft. This provides for a very slowly changing and otherwise benign thermal environment. The effect of the rotation on the operations is to move the star field image to different CCDs within the focal plane every three months and then begin a new three-month period with the stars imaged on a new fixed set of pixels. This causes only a small loss of transit data during the time of the rotation and restabilization (about a day). There is no requirement for the baselines before and after the rotation to match. To demonstrate that the noise and ability to detect transits is not dependent on any one unique set of pixels or location on the CCD, the image was translated from one end of the CCD furthest from the readout registers to the end nearest the readout registers. The resulting performance, which is actually better than baseline, is shown in Figure 4b. For the remainder of the tests the image was shifted back to the far end of the CCD.

4.3. Impact of bright stars

For the large star field that will be viewed during the *Kepler Mission* there will be 15 stars as bright as 4^{th} to 6^{th} magnitude. To test the impact of these bright stars, a 4^{th} magnitude bright star was introduced into the test image. The result of this test is presented in Figure 4c. One star (far upper-left corner in Figure 4c) that was particularly close to the column containing the bright star not only had significantly more noise, but its apparent brightness was about one stellar magnitude brighter. Thus, the bright star only adversely affects a few columns of the CCD and thereby causes only a small loss of usable stars. Aside from a few stragglers, the overall noise is still well below the max-allowed.

4.4. Spacecraft jitter of 10x nominal

Based on previous spacecraft performance data and engineering modeling done by Ball Aerospace & Technologies Corporation for the *Kepler Mission,* an estimate of the three-sigma pointing stability of ±0.03 arcsec has been derived. The PZTs in the Testbed were driven at the frequencies and at ten times the amplitude prescribed by this attitude control system model. The result of this test is presented in Figure 4d. Except for a few stragglers, the overall noise is still well below the max-allowed even at ten times nominal spacecraft jitter.

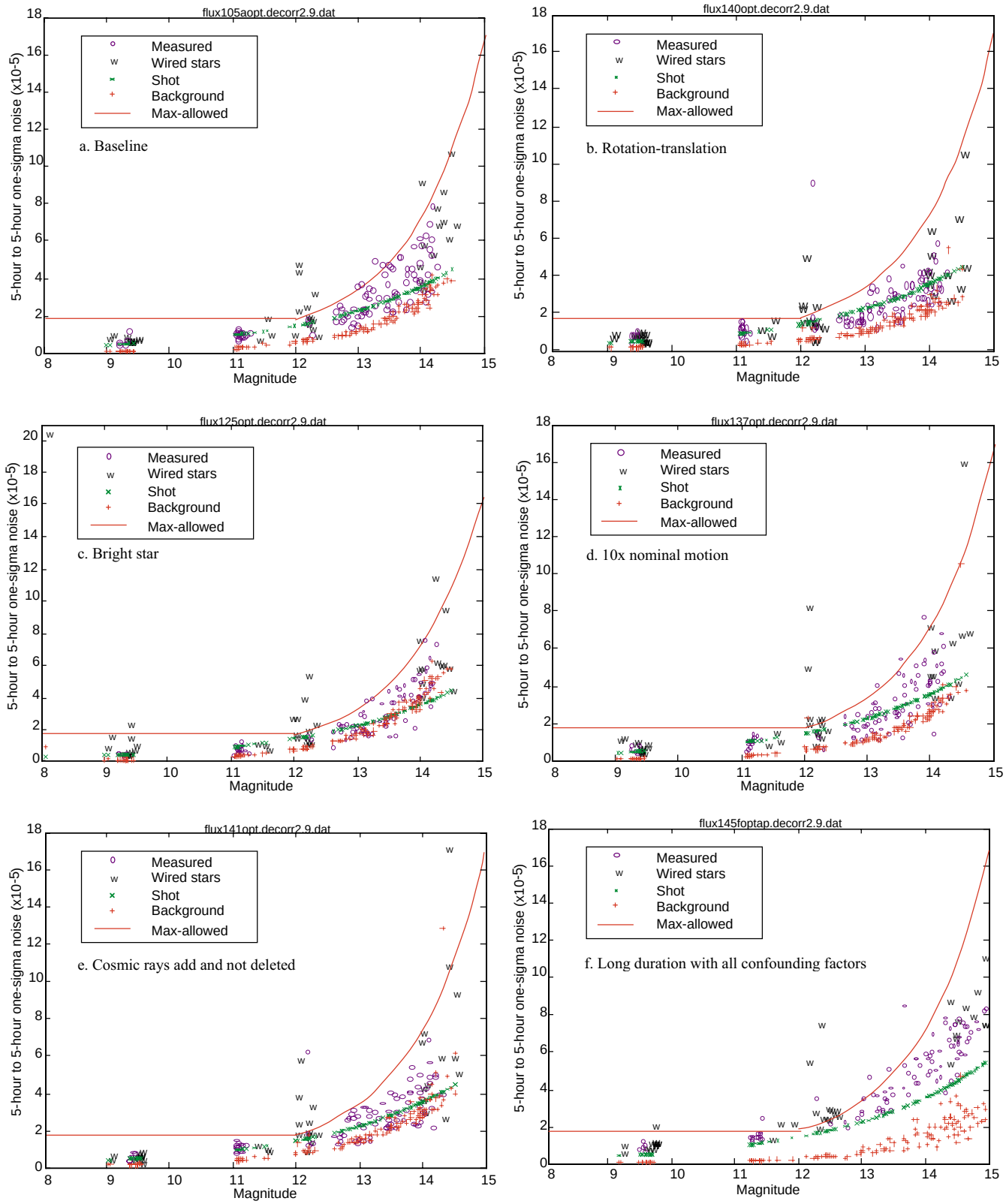

Figure 4 Test results for inclusion of various individual and combinations of noise sources. The measured values for stars with wires are shown with a W. The transit wires themselves induce added noise to those stars. The max-allowed is the total allowed for all instrument noise sources plus shot noise for the mission to meet its objectives. The average total noise is well below the max-allowed line. Note, the scale is slightly different for plot c.

4.5. Cosmic rays

Cosmic ray hits have nearly always been detrimental to photon detectors. They cause both radiation damage and deposit energy. Over an extended period of time, CCDs produce traps, hot pixels, increased dark current and reduce the charge transfer efficiency[9] (CTE). They also deposit unwanted charge when they interact. Radiation damage is a common problem for all CCD uses, has been a topic of continual study and may be mitigated to some extent by charge injection sometimes called a "fat zero". The fat zero also adds extra shot noise which is an issue in low-flux situations. For the *Kepler Mission*, there is no shutter. Hence, the smearing of stars acts like a fat zero and has the beneficial side effect of keeping the traps filled. Long-term radiation damage has not been incorporated into this Testbed. Charge deposited by cosmic rays is particularly problematic when using the CCD to measure very low fluxes[10, 11]. A cosmic ray may deposit more charge in one instant than is normally expected for a long exposure. However, to achieve the low shot-noise level for the *Kepler Mission*, $>3x10^8$ electrons per five hour integration are required for even the faintest star (m_V=14), so that cosmic rays do not appear to be a major source of additional noise. To test this, the equivalent of a Baseline test was run in which simulated cosmic rays were injected into the 3-second readouts based on a model for the comic ray flux seen in the LASCO/SOHO instrument[12]. The cosmic-ray flux corresponded to 6 /cm^2/sec with 2500 e$^-$ on average deposited in a pixel[13]. The result of this test is shown in Figure 4e. Again, aside from a few stragglers, the overall noise is still well below the max-allowed.

4.6. Long-duration confounding-factors test

After performing the various tests to identify any adverse effects of any individual source of noise, a long-duration test was performed, which incorporated all of the confounding factors using nominal values. That is, in addition to those incorporated in the Baseline test, this test included a bright star at 4th magnitude, nominal spacecraft jitter and cosmic rays. In this test the cosmic rays were injected but **not** removed. The results for ten days of this test are presented in Figure 4f. Again there are several noisy W-stars. In addition the overall noise level is somewhat higher than in any other test with several stars deviating above the max-allowed line. However, note that these few stragglers do not raise the ensemble average above the max-allowed line.

4.7. Test summary

In all of the tests performed, the noise level was below the maximum allowed, with the exception of those stars that had transit wires. A tabular summary of the fractional measured noise in units of 10^{-5} is given in Table 3. The max allowed noise is from Table 1 line 5, where the required value for stars brighter than 12th magnitude is taken to be no better than that for 12th. The 13th mw and 14th mw are those stars that are in the crowded region representative of the star field density in the Milky Way where the *Kepler Mission* will be observing.

Table 3 Summary of Test Results, Average Measured Total (Shot and Instrument) Noise (x10^{-5})

Stellar magnitude	9th	11th	12th	13th	14th	13th mw	14th mw
Max allowed noise (RSS shot and instrument)	1.68	1.68	1.68	3.28	7.20	3.68	7.28
Baseline test	0.48	0.72	1.60	2.64	3.44	2.96	5.84
Rotation/translation test	0.40	1.20	1.04	1.68	2.72	2.00	2.96
Bright star test	0.40	0.96	1.60	2.24	4.80	3.12	6.88
Motion at 10x nominal	0.40	0.96	1.44	2.24	7.36	2.72	4.88
Cosmic ray test	0.40	0.64	1.36	1.60	5.36	2.16	3.36
Long duration, all confounding factors	0.56	1.20	1.44	2.56	6.16	3.20	4.80

4.8. Transits

Earth-size transits cause a very small change in brightness ($8x10^{-5}$) for several hours on individual stars. Although the noise performance of the system is important, the most critical requirement is to be able to detect Earth-size transits.

4.8.1. Transit generation

An innovative way to simulate transits is used to produce this small change. A fine fixed wire is mounted across the star hole (see Figure 5). To produce the required small change in the brightness of the star hole, a current is passed through the wire. The resistivity of the wire causes it to heat to a few degrees above ambient. The desired temperature rise is on the order of 5°C. Due to the small coefficient of thermal expansion of the wire, the wire expands by 2 nm/°C and blocks the required fraction of light. Transit wires are mounted across 42 of the star holes, but only about a dozen are used during any one test and only one transit is on at any given time. The switching on and off and monitoring of the transits are performed with a Macintosh computer running LabView software. Figure 5 shows the completed star plate assembly.

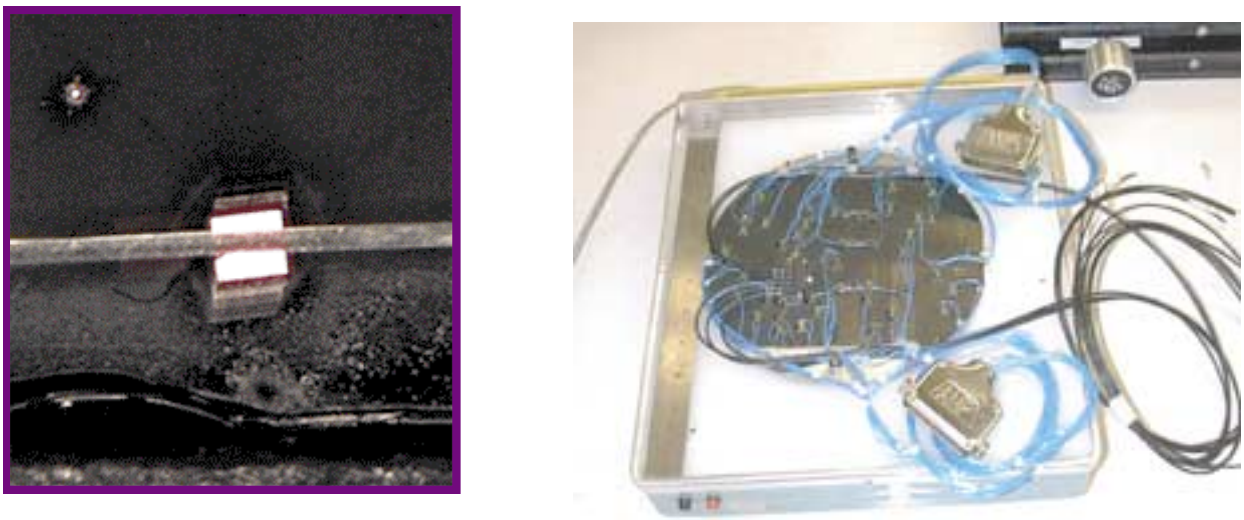

Figure 5 On the left is shown a transit wire on an m_V=9 star hole with an m_V=14 nearby background star in the upper left. On the right is shown the completed star plate with 1600 laser drilled holes, 42 transit wires and 5 fiber optic bundles for bright stars.

4.8.2. Transit detection

Transit events measured with the Testbed Facility from the long-duration test with all confounding factors are shown in Figure 6 for m_V=9, 12 and 14 stars. The transit depths are given in Earth-area. The error bars are for ±1σ. The long-duration test demonstrated multiple detections of periodically applied 5-hour transits as well as detection of a simulated 12-hour transit. In the previous 48-hour tests there were typically ten individual transits applied to different stars. At least 90% were detected with the required SNR. The cause of the relatively few missed transits was additional noise produced by the transit devices themselves and does not reflect on the ability of the actual spaceborne photometer to detect nearly 100% of transits of comparable size.

5. CONCLUSIONS

The *Kepler Mission* is designed to detect hundreds of Earth-size planets by looking for transits. To demonstrate the technology to be utilized, a Testbed Facility has been built and operated with a flight-type CCD. The facility simulates all of the features of the sky and the spacecraft/photometer that are important for the success of the mission. Optimum operating conditions for the PSF, photometric aperture size versus stellar brightness, and maximum operating temperature have been

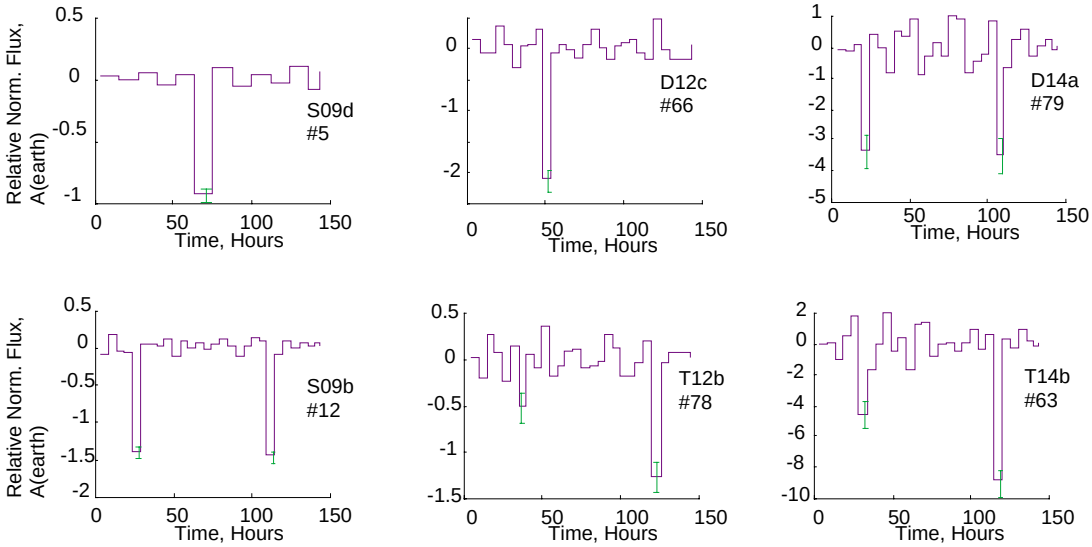

Figure 6. Transits produced and detected during the running of the long-duration test with all confounding factors. Transit depth is given in equivalent Earth-sizes and one sigma error bars are shown for the noise. The left two transits are for 9th magnitude stars, the center two for 12th magnitude stars and the right two for 14th magnitude stars. At 14th magnitude the minimum detectable planet size is 1.9 Earth-radii due to a higher shot noise (see Table 1 line 7).

measured. Proto-flight software necessary for processing the data has been utilized throughout. The required photometric precision has been demonstrated while operating without a shutter during readout, having some saturated pixels in the brightest stars, working in a crowded field with a star density the same as planned for the mission, inclusion of spacecraft jitter, and over a dynamic range of five stellar magnitudes. Additional tests of comic-ray hits and field rotation also do not have detrimental effects. Transits have been injected and detected at the required statistical significance under all operating conditions during all tests.

In a long duration test of greater than ten days the Camera was simultaneously subjected to normal tracking errors, uncorrected cosmic ray hits, a 4^{th} magnitude star in the CCD field, and all of the other confounding factors expected under realistic operating conditions. These tests demonstrated that SNRs of 4.6 are achievable for Earth-size transits of 9^{th} to 12^{th} magnitude stars without stellar variability, permitting SNRs of 4.0 when stellar variability is included. For 13^{th} and 14^{th} magnitude stars the SNRs (including variability) are 2.3 and 1.1, respectively, due to the higher level of shot noise.

While the achievement of 10^{-5} precision had already been demonstrated in earlier tests, the results presented here provide ample evidence for the ability of existing commercially available CCDs in an end-to-end test with realistic operating conditions to consistently achieve a fractional precision of better than $1x10^{-5}$ and to consistently detect simulated Earth-size transits at the require SNR. The very successful test results should greatly reduce any perceived risk in the Kepler approach to planet detection.

ACKNOWLEDGMENTS

Support for this project was received from NASA Ames Strategic Investment Funds for purchase of the CCD, from NASA's Origins program (UPN 344-37-00) for development of the Camera and from NASA's Discovery program and Ames Research Center for construction and operation of the Testbed Facility and analysis of the data. Special thanks go to the team that made the demonstration successful, especially, Tom Conners for the mechanical design and fabrication, Bob Hanel for the electrical design and fabrication, Larry Kellogg for the Labview programming, Chris Koerber for the transit wire assembly, facility assembly and overall technical support, Scott Maa for the thermal design and Brian Taylor for development and refinements of the LOIS software. The guidance, criticism and recommendations of the Technical Advisory Group, Tim Brown, John Geary and Steve Howell, were very much appreciated. Finally the authors acknowledge the continued support of the *Kepler Mission* by all levels of Ames Research Center management.

REFERENCES

1. Charbonneau D., Brown, T. M., Latham, D. W. and Mayor, M., ApJ Lett, in press, (1999)
2. Borucki, W. J., Koch, D. G., Dunham, E. W., and Jenkins, J. M.,The Kepler Mission: A Mission to Determine the Frequency of Inner Planets Near the Habitable Zone of a Wide Range of Stars, *Planets Beyond The Solar System and The Next Generation of Space Missions, ASP Conf Ser* ,**119**, 153-173 (1997), ed. David Solderblom
3. Koch, David, Borucki,William, Webster,Larry, Dunham,Edward, Jenkins,Jon, Marriott, John and Reitsema,Harold, *Space Telescopes and Instruments V SPIEConference* **3356**, , 599-607 (1998)
4. Robinson, L. B, M. Z. Wei, W. J. Borucki, E.W. Dunham, C. H. Ford, and A. F. Granados. *PASP* **107**, 1094-1098 (1995)
5. Jenkins, Jon M., Borucki, William J., Dunham, Edward W. and McDonald, John S., High Precision Photometry with Back-Illuminated CCDs, *Planets Beyond The Solar System and The Next Generation of Space Missions, ASP Conf Ser* ,**119**, 227-280 (1997) ed. David Solderblom
6. Jon M. Jenkins, Fred Witteborn, David G. Koch, Edward Dunham, William J. Borucki, Todd F. Updike, Mark A. Skinner, and Steve P. Jordan, Processing CCD images to detect transits of Earth-sized planets: Maximizing sensitivity while achieving reasonable downlink requirements, (these proceedings)
7. Taylor, B. W., Dunham, E. W., Gould, A., Osip, D. J., and Elliot, J., L., Lowell Observatory instrument system (LOIS): a modular control system for astronomical instrumentation, *SPIE Conf* **4009**. (2000)
8. Leach, Robert, CCD Controller Requirements for Ground-based Optical Astronomy, Solid State Sensor and CCD Cameras *SPIE* **2654,** 218-225 (1996)
9. Whitmore, Heyer, and Casertano, Charge Transfer Efficiency of WFPC2, *PASP* **111**, 1559-1576 (1999)
10. Windhorst, R. A., Franklin, B. E. and Neuschaefer, L. W., Removing Cosmic-Ray Hits from Multiorbit HST Wide Field Camera Images, *PASP*, **106**, 798-806 (1994)
11. Slazberg,S., Chandar, R., Ford, H., Murthy, S., and White, R., Decision Trees for Automated Identification of Cosmic-Ray Hits in Hubble Space Telescope Images, *PASP*, **107**, 279-288 (1995)
12. R. A. Howard, private communication (1998)
13. Gilliland, R. L., Edmonds, P. D., Petro, L., Saha, A., and Shara, M. M., *Ap. J. Lett.*, **447**, 191-203, (1995)